

Content-Preserving Image Stitching with the Regular Boundary Constraint

Yun Zhang, Yu-Kun Lai, *Member, IEEE*, and Fang-Lue Zhang, *Member, IEEE*

Abstract—This paper proposes a content-preserving stitching with the regular boundary constraint, which aims to rectanglizing the panorama images with irregular boundary, while avoiding unexpected distortions in the warping-based processes. In our method, the traditional stitching is improved by considering the regular boundary constraint, and the stitching process is configured to be a two-step global optimization which can be efficiently solved. We first conduct stitching by traditional warping-based optimization, and take the warped meshes as initial conditions of the final stitching. Then, we obtain the irregular boundary from the warped meshes by the polygon boolean operations, and construct piecewise rectangular boundary by analyzing and sorting vertices on the irregular boundary. With the piecewise rectangular boundary constraint, we proceed the second step global optimization which incorporates straight line preserving and regular boundary constraints into the image stitching framework. We further conduct iterative optimization to obtain optimal piecewise rectangular boundary, thus can make the panoramic boundary be close to rectangle as much as possible, while reducing unwanted distortions. We further extend our method to panoramic videos and selfie photography, which integrate the temporal coherence and portrait-preserving into the optimization. Experiments show that our method can efficiently produce visual-pleasing results with regular boundaries, unnoticeable distortions.

Index Terms—content-preserving, panorama, irregular boundary, piecewise rectangular, warping.

1 INTRODUCTION

THE rapid recent advances in digital visual media mean that the public now capture and produce high-quality images and videos, which has promoted the computer graphics applications that utilise visual data captured by ordinary users. Image/video panorama is one of these successful applications. With the integrated panorama module in their smart phones and portable cameras, people can easily take a panoramic photos simply by moving cameras. It is also the most feasible way to get virtual reality content for immersive vision experiences. However, unlike the well calibrated images captured by professional devices with a camera array, the intrinsic and extrinsic parameters of the images captured by consumer-level devices are difficult to estimate. Thus, a robust image stitching method which directly stitches using the visual content is much more important for the applications designed for the ordinary users,

Recently, a lot of progresses have been made in image stitching. However, due to the casual motion of the handheld cameras, after feature alignment, most stitching results by previous methods have irregular boundaries. To display the full panorama in common screens, or generate free-viewpoint photos from one part of the whole scene recorded by the image collection, we can only show them in rectangular windows.

A simple and direct method is cropping, but it will lose important content of stitched panorama, thus may reduce the impression of wide angle photography. In order to produce panorama images with rectangular boundaries, image completion techniques [1], [2] are used to synthesise the missing region in the panorama's bounding box. However, these methods are not stable, and may fail when there need to be semantic meaningful objects. He et al. [3] proposed a warping based method to rectanglizing panorama images, which can stably produce visual-pleasing panorama images with rectangular boundaries. But their method suffers from the following problems: (1) The stitching and rectanglizing are two separated processes, so the latter rectanglizing step may twist the optimized stitching result, making it hard to get an optimal rectangle panorama. (2) When placing grid meshes in stitched irregular panoramas for rectanglizing, boundary meshes may contain small holes, see Fig. 3(c). (3) The warping-based method will produce large distortion and destroy the feature alignment, when the scene is not completely shot. Thus, when the gap between the rectangular boundary and irregular panorama boundary is large, or there are holes which are difficult for completion and warping methods to fill, there need to be a better approach to create the panorama with regular boundaries while avoiding distortions.

In this paper, we propose a content-preserving image stitching, which aims to regularize the boundary of stitched panorama, and preserve as much as possible content in a rectangular cropping window. Our method can also be applied in videos and selfie photography, and can produce panorama video and selfie with regular boundary. Similar to He et al. [3], the process of generating panorama images with rectangular boundaries is termed as “rectanglizing”. Our method is based on the following observations: (1) Rect-

- Yun Zhang is with the Institute of Zhejiang Radio and TV Technology, Communication University of Zhejiang, Hangzhou, China, 310018.
E-mail: zhangyun@cu.edu.cn
- Yu-Kun Lai is with the School of Computer Science and Informatics, Cardiff University, Wales, UK, CF24 3AA.
E-mail: Yukun.Lai@cs.cardiff.ac.uk
- Fang-Lue Zhang is with the School of Engineering and Computer Science, Victoria University of Wellington, New Zealand.
E-mail: fanglue.zhang@ecs.vuw.ac.nz

angling and stitching are tightly related, and combination of the two processes may help to produce better rectangling panorama in a content-aware manner. (2) The aim of panorama rectangling is to preserve as much as possible image content in a rectangular window while avoiding unexpected distortion, thus the irregular boundary should not be simply optimized to be a single rectangle, but piecewise rectangle, see Fig. 2(c).

Our method works well in a variety of cases, and can produce visual-pleasing results with no user interactions. The key idea of our algorithm is a two-step optimization. We first stitch images using traditional method to get irregular boundaries, and then we extract and outer boundary and analyze the boundary constraint, finally we globally optimize the mesh to get stitching results with regular boundaries. In the first step, we apply image stitching with the global similarity prior [4], and get the boundary vertices by the polygon boolean union operation. In the second step, We extract the irregular boundary by the polygon boolean operations, and then construct the regular boundary constraint by analyzing the vertices and intersections in the irregular boundary. Finally, we design a global optimization which takes into account the regular boundary, shape preserving, straight lines, global similarity constraints. When the target boundary is simply a rectangle, see Fig. 1, the panorama image is directly obtained by solving the global optimization. For panorama shot by freely moving cameras, the target boundary can not simply represented by a rectangle, see Fig. 2, and we propose piecewise rectangle to represent the regular boundary. With the new boundary condition, we get the panorama by solving the optimization and warping. Then we iteratively combine boundary segments connected by *step*(see Fig. 1(f)), and finally we get panorama image with optimal piecewise rectangular boundary. Our final result can help users easily crop panorama while preserving as much as possible content in the cropping window, while avoiding unwanted distortions and enhancing the panorama viewing experiences.

Contributions of this paper are as follows:

- We propose a global optimization to solve the irregular boundary problem in traditional stitching framework by considering the regular boundary constraint, and further apply our method to panoramic selfie and videos.
- We propose a piecewise rectangling scheme to make the panoramic boundary close to a rectangle as much as possible, while avoid unexpected distortions.

2 RELATED WORK

In this section, we briefly review the most related works.

image stitching. Image stitching aims to create seamless and natural photo-mosaics, and a comprehensive survey of image stitching algorithms is given in [5]. Brown et al. [6] proposed fully automatic panoramic image stitching, and align multiple images by a single homography. Their method is effective under assumption that camera only rotates around its optical center, images are shot from the same viewpoint and the scenes are nearly planar. However, for images shot by hand-held cameras always contain parallax, which limits the application of their method. Given

the limitation of single homography, Gao et al. [7] proposed to use two homographies to perform nonlinear alignment, when the scene is modeled by dominant distant and ground planes. However, their method is only effective when there is no local perspective variations. For better performance in image alignment, Zaragoza et al. [8] proposed as-projective-as-possible(APAP) warps based on moving DLT, and can seamlessly align images with different projective models. Their method can achieve globally perspective, while allowing local non-projective deviations, thus can deal with some challenging cases. Now APAP [8] has been widely applied for its excellent performance in accurate alignment. In this paper, we also apply APAP for image alignment in stitching. Based on the accurate alignment in APAP [8], Lin et al. [9] combined local homography and global similarity transformation to achieve more continuous and smooth stitching, and provided more natural panorama with less visible parallax and perspective distortion. Li et al. [10] proposed dual-feature warping-based model by combining keypoints and line segment features. However, the 2D model proposed in this paper cannot handle large parallax and depth variation, and it is difficult to determine the line correspondences in images with large parallax. For natural warping in stitching, Chang et al. [11] proposed a parametric warp which combines projective and similarity transformation. By combining APAP [8], their method can provide more accurate alignment, less distortion. Chen et al. [4] proposed natural image stitching with global similarity prior to reduce distortion while keep good alignment. To preserve global similarity, they further proposed schemes to select proper scale and rotation for more natural stitching results. To stitch images with large parallax, Zhang et al. [12] proposed local stitching method, which is based on the observation that overlapping regions do not need to be aligned perfectly. Lin et al. [13] proposed a seam-guided local alignment, and optimal local alignment is guided by the seam estimation. In their method, salient curve and line structures are preserved by local and non-local similarity constraint. Very recently, Li et al. [14] proposed robust elastic warping for parallax-tolerant image stitching. To ensure a robust alignment, they proposed a Bayesian model to remove incorrect local matches. He et al. [3] proposed a content-aware warping to produce rectangular images from stitched panorama. Their method is effective to rectangling irregular boundaries caused by projections and casual camera movements. However, their two-step warping strategy separates stitching and rectangling process, which can not ensure an optimal solution, and their method can not process panoramic scenes that are not completely shot. Inspired by [3], We incorporate rectangling into the stitching framework, and construct global optimization to get rectangular panoramic images. We also proposed solutions to deal with challenging cases, such as images that are not completely shot, and apply our method to panoramic videos and selfies.

video stitching. Compared with image stitching, video stitching is much more difficult, due to the camera motion, dynamic foreground and large parallax. For static camera settings, such as multi-camera surveillance [15], [16], videos from different cameras are aligned only once, and the main challenge is to avoid ghosting and artifacts caused by moving objects. For moving cameras with rel-

ative fixed positions, such as camera arrays fixed on the rig [17], cameras can be pre-calibrated for global stitching of videos, and spatio-temporally coherent warping, minimal distortion are the main challenges due to the motion and parallax. Google streetview [18] also applies moving camera arrays for street view capture and panorama generation. To generate high-quality panorama videos, for videos captures by camera arrays fixed on a rig, Zhu et al. [19] proposed realtime panorama video blending. Meng et al. [20] proposed multi-UAV surveillance system that supports real-time video stitching. Recently, many researchers focus on stitching algorithm for videos shot by multiple hand-held cameras. El-Saban et al. [21] proposed optimal seam selection blending for fast video stitching, however, they do not consider video stabilization. Lin et al. [22] firstly proposed robust framework stitch videos from moving hand-held cameras, which incorporates stabilization and stitching into a unified framework. Guo et al. and Nei et al. [23], [24] further improve the performance of jointly video stabilization and stitching framework. Their main contributions include: estimation of inter motions between cameras and intra motions in a video; common background identification for multiple input videos. In this paper, we extend our content-preserving image stitching to videos that are captured from unstructured camera arrays [17].

3 OVERVIEW

Fig. 1 gives the pipeline of our content-preserving stitching. The input to our approach is a number of images with content overlaps, and the goal is to obtain panorama images with regular boundaries by our content-preserving stitching. We first perform traditional image stitching, and extract the irregular boundary by polygon boolean operations. Then, we further analyze and sort vertices on the irregular boundary, and construct the piecewise rectangular boundary constraints. With the boundary constraint above, we obtain the piecewise rectangling result by iteratively solving global optimizations. We place quad-mesh on each image, and construct energy functions with constraints on the mesh. After optimization, the stitching results are rendered by image warping and blending. The core of our approach is the unified optimization framework that combines image stitching and rectangling, which contains following steps:

Preprocessing. In this step, we first calculate the image match graph using the method proposed in [6], and images that are connected in the match graph are aligned to be panoramas. This automatic match process allows stitching with complex image overlaps. For straight line and global feature preserving, we detect lines in all images using fast line segment detector [25].

Initial image stitching. The goal of this step is to initialize our content-preserving stitching, and our regular boundary constraints are based on the analysis of warped meshes after stitching. The stitching strategy in this step is also applied in our global optimization which combines stitching and rectangling. We apply APAP [8] for accurate feature alignment. Inspired by [4], we also add a global similarity term for more natural stitching, and the distortion is minimized globally.

Irregular boundary extraction. After the initial image stitching, we extract the contour of each warped mesh, and get the irregular boundary by the polygon boolean Union operation. Then, we analyze and sort vertices and intersections on the irregular boundary. Finally, we set the target rectangular boundary constraints for our piecewise rectangular stitching.

Piecewise rectangular stitching With the rectangular boundary constraints above, we construct energy optimization which contains image stitching and regular boundary constraint. After minimizing the energy function, we get the stitching result by warping and blending. We iteratively optimize the stitching result by combining boundary segments near the cuts of each direction.

4 CONTENT-PRESERVING IMAGE STITCHING

In this step, we propose a global optimization which aims to generate panoramas with regular boundaries in the image stitching framework. The optimization consists of the following constraints: feature alignment, shape preserving, global similarity preserving, straight lines preserving and regular boundary constraints. With the optimized vertices, we warp the mesh by texture mapping, and remove the seams by multi-banded blending. For scenes that are not completely shot, our piecewise rectangular stitching can iteratively optimize the target panorama boundary, and make the shape of our panorama be close to a rectangle as much as possible, while avoiding the unwanted distortions.

4.1 Initial image stitching

In this step, images are stitched using traditional method, and the irregular boundary of warped mesh are initial conditions for our piecewise rectangular stitching. Actually, when the gap between the irregular boundary and the target rectangular boundary is too large, it will be difficult or even impossible for rectangling with unnoticeable distortion. Inspired by [4], we stitch images using the global similarity prior to generate more natural panoramas without too much distortions and limit of field of view. Like previous methods, image stitching is performed by mesh-based image warping. Let V_i and E_i be the vertices and edges in image I_i , we aim to get deformed vertices V by minimizing the energy function $\Phi(V)$, which contains following terms: Feature alignment, local shape and global similarity preserving.

Feature Alignment. This term aims to align matched images by preserving the feature correspondences between them. Given the good performance in piecewise alignment, we apply APAP [8] for feature alignment, and the feature alignment constraint is defined as follows.

$$\phi_a(\mathbf{V}) = \sum_{i=1}^N \sum_{(i,j) \in G} \sum_{p_m^{ij} \in M_{ij}} \|\mathbf{V}_{pq}^{ij} \cdot \boldsymbol{\Omega}_{pq}^{ij} - \tilde{\mathbf{V}}_{pq}^{ij} \cdot \tilde{\boldsymbol{\Omega}}_{pq}^{ij}\|^2, \quad (1)$$

where G refers to the image match graph which determine the matched image pair. p_m^{ij} represents a pair of matched feature points in image i and j respectively, and M_{ij} is the image matching set. Since the constraints are imposed

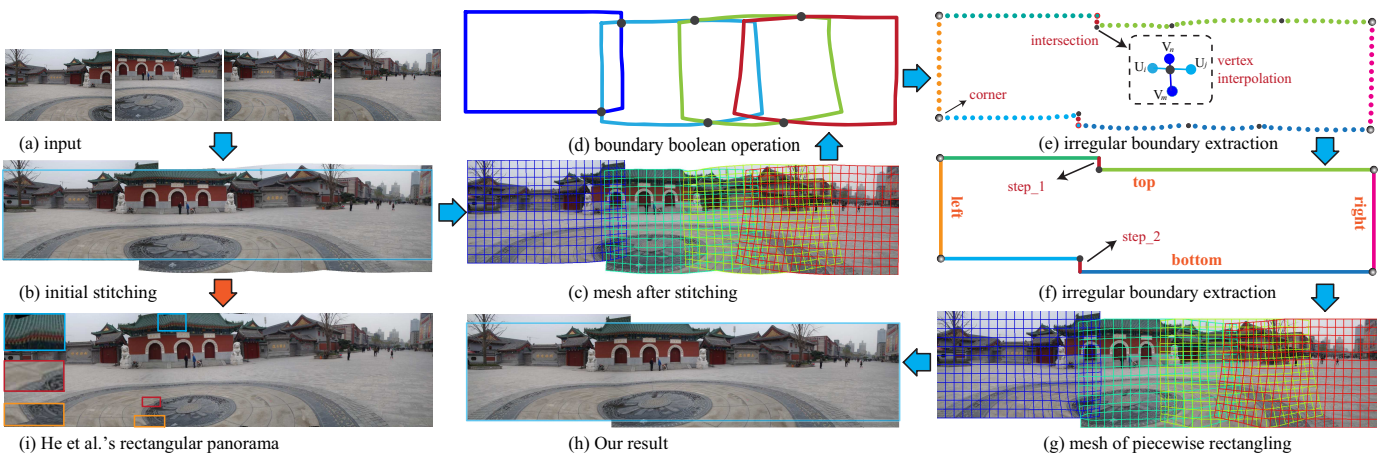


Fig. 1. Pipeline of our stitching with regular boundary. (a) Input images. (b) initial stitching with irregular boundaries. (c) mesh of initial stitching. (d) outer boundary extracted by polygon boolean extraction. (e) irregular boundary extraction. (f) target regular boundary. (g) mesh of piecewise rectangling. (h) our result. (i) He et al.'s rectangular panorama.

on vertices of the mesh, we employ the bilinear coordinates represent matched feature points as the interpolation of four vertices of a quad grid $p_{ij}^m = \mathbf{V}_{pq}^{ij} \cdot \Omega_{pq}^{ij}$, where $\mathbf{V}_{pq}^{ij} = [V_{p,q}^{ij}, V_{p+1,q}^{ij}, V_{p+1,q+1}^{ij}, V_{p,q+1}^{ij}]$ and $\Omega_{pq}^{ij} = [\omega_{p,q}^{ij}, \omega_{p+1,q}^{ij}, \omega_{p+1,q+1}^{ij}, \omega_{p,q+1}^{ij}]$.

Shape consistency. This term aims to ensure that each quad grid in the mesh can undergo a similar transform and do not distort too much. we use the shape preserving term defined in [26], which split each grid into two triangles and applies the method in as-rigid-as-possible warping [27].

$$\phi_s(\mathbf{V}) = \sum_{i=1}^N \sum_j \|V_j^i - V_1^i - \xi \mathbf{R}(V_0^i - V_1^i)\|^2, \quad (2)$$

where $\mathbf{R} = \begin{bmatrix} \cos\theta & \sin\theta \\ -\sin\theta & \cos\theta \end{bmatrix}$,

and $\xi = \|V_j^i - V_1^i\| / \|V_0^i - V_1^i\|$.

In Equ. 2, θ refers to the angle formed by moving segments From $V_1 V_0$ to $V_1 V$, when the direction is anticlockwise $\theta = 90^\circ$, and $\theta = -90^\circ$ for the clockwise direction. In our implementation, V_j^i refers to the top-left vertex of all quads in the image mesh, V_0^i and V_1^i are the neighboring vertices of V_j^i in a triangle.

Global similarity. We use the global similarity term proposed in [4], which is important to preserve the naturalness of the panorama images. We first set a reference image I_0 and its desired rotation r_0 , then for each image desired scale s_i and rotation r_i with respect to I_0 are calculated, see details in [4]. The global similarity term is defined as

$$\phi_g(\mathbf{V}) = \sum_{i=1}^N \sum_{e_j^i \in \mathbf{E}_i} \alpha(e_j^i) [||c(e_j^i) - s_i \cos\theta_i||^2 + ||s(e_j^i) - s_i \sin\theta_i||^2], \quad (3)$$

In Equ. 3, $c(e_j^i)$ and $s(e_j^i)$ refer to the coefficients of grid edges for similarity transform in x and y directions, see details in [28]. $\alpha(e_j^i)$ is the weight to assign more importance to the edge in the overlapping region, while less in other

area, in order to keep accurate alignment and preserve the naturalness, and it is defined as

$$\alpha(e_j^i) = \frac{\sum_{q_m \in Q(e_j^i)} \text{Min}(d_{cen}(q_m, \Psi_i))}{\sqrt{W_i^2 + H_i^2} \cdot |Q(e_j^i)|}, \quad (4)$$

where $Q(e_j^i)$ refers to the quads that contains edge e_j^i ; Ψ_i is the overlap region in Image I_i ; $\text{Min}(d_{cen}(q_m, \Psi_i))$ calculates the minimum distance between the center of quad q_m to quads in Ψ_i ; W and H are the number of rows and columns in the mesh of image I_i .

With the energy terms defined above, we define the optimization for image stitching as

$$\Phi_{stitch}(V) = \arg \min_V (\gamma_a \phi_a(\mathbf{V}) + \gamma_s \phi_s(\mathbf{V}) + \gamma_g \phi_g(\mathbf{V})). \quad (5)$$

In Equ. 5, there are three weights γ_a , γ_s , γ_g , which controls the importance of the three terms. In our experiments, we set $\gamma_a = 1.5$, $\gamma_s = 10$, $\gamma_g = 0.75$ for most of the cases. The stitching energy $\Phi(V)$ are quadratic and can be efficiently minimized by solving a sparse linear system.

4.2 Irregular boundary extraction

For panorama rectangling, we need to drag the vertices on the irregular boundary onto the regular boundary. Different from [3], which place only one mesh. In our method, the irregular boundary consists of vertices from different image meshes, and there also exists some intersections in the overlapping regions, see the second row of Fig. ??(c). Inspired by the boolean operations on polygons [29], We propose a simple and effective algorithm for irregular boundary construction. See Alg. 1, the input is the mesh vertices \mathbf{V}_i of each warped image I_i , and the goal is to get index of boundary vertices and the directions to be dragged. We first get minimum outer rectangle R of all warped meshes, and search 4 corners of irregular boundaries according to the minimum distance between corners of each mesh \mathbf{V}_i and R . Then, we construct polygons ϑ using the contours of each mesh, and the irregular boundary P can be efficiently calculated by the polygon boolean union operation of all boundary polygons. With corners Δ and boundary polygon P ,

the boundary vertices of 4 directions can be easily obtained by sequentially collecting vertices between neighboring corners of P . As shown in Fig. ??, the initial image stitching result has irregular boundary which is the combination of 4 meshes. (b) shows contours of all meshes, and each contour has a different color. the black circles are intersections of these contours. As shown in (c), After the polygon boolean union operations, the irregular boundaries are correctly sorted. With the detection of four corners, boundary vertices (including intersections) are easily detected and classified into 4 directions. For the intersection points, which cannot be constrained as vertices. We first detect the corresponding intersected vertices κ , and calculate the interpolation weight of the vertices η , then the intersection points can be easily constrained by the neighboring vertices.

Algorithm 1: Irregular boundary extraction

Input: Mesh vertices \mathbf{V}_i of each warped image I_i ,
 $i = 1, 2, \dots, N$
Output: Index of boundary vertices \mathfrak{R} and their labels
 ζ

Get minimum outer rectangle R of all meshes;
Set $D_{min} = Dist(Corners(R), Corners(\mathbf{V}_i))$;
construct polygon ϑ_1 using contour vertices of mesh \mathbf{V}_i ;
Set $P = \vartheta_1$;
Set boundary corners $\Delta = Corners(\mathbf{V}_1)$;
for ($i = 2; j \leq N; j++$) **do**
 Construct polygon ϑ_i using contour vertices of I_i ;
 Polygon boolean Union: $P = P \cup \vartheta_i$;
 if ($dist(Corners(R), Corners(\mathbf{V}_i)) < D_{min}$) **then**
 $\Delta = Corners(\mathbf{V}_i)$;
 $D_{min} = Dist(Corners(R), Corners(\mathbf{V}_i))$;
 end
end
for ($j = 1; j \leq size(P); j++$) **do**
 if ($P[j] \in vertices$) **then**
 $\zeta[P[j]] = 1$;
 end
 else if ($P[j] \in intersections$) **then**
 $\zeta[P[j]] = 0$;
 $\kappa[P[j]] = [V_m, V_n, V_p, V_q]$;
 $\eta[P[j]] = [C_m, C_n, C_p, C_q]^T$;
 end
end
Get boundary vertices between neighboring corners of P ;
for ($k = 1; k \leq 4; k++$) **do**
 $\mathfrak{R}(k) = P(\Delta(k), \Delta((k+1)\%4))$;
end

4.3 Piecewise rectangular boundary constraint

For panoramic scenes with missing content, He et al.'s [3] warping-based rectangling cannot work well, as it may introduce unexpected distortions, see Fig. 1(i). Actually, panorama images with irregular boundary cannot simply be warped to be a rectangle, and the rectangling process should be content-preserving. In this paper, we propose

to the piecewise rectangular boundary which makes the target boundary as rectangular as possible, while avoiding the unwanted distortions. See Fig. 1(h), with the piecewise rectangular boundary, the stitching result can be cropped easily, while preserving more content in a cropping window.

Alg. 2 gives details of piecewise regular boundary analysis. The input is mesh vertices of irregular boundaries V^i , and the output is the segmented boundary S^i , $i = 1, 2, 3, 4$ refers to index of 4 directions. The irregular boundaries are comprised of boundary vertices from different image meshes, which are connected by their intersections. We first segment the V_i by intersections and corner vertices (with red boundary in Fig. 1(e)) of each mesh. Then we combine neighboring segments with the same direction, and incorporate segments with less than 3 vertices into previous segment. After sorting the irregular boundaries, we calculate the target boundary value of each segment by averaging their coordinates in corresponding direction. See Fig. 1(f), the top and bottom boundary contain 3 segments, and the steps are designed to reduce distortions in global warping.

Algorithm 2: Piecewise regular boundary analysis

Input: Mesh vertices \mathbf{V}^i of irregular boundaries,
 $i = 1, 2, 3, 4$ refer to 4 directions(T/R/B/L)
Output: Segmented boundary S^i , includes vertices,
directions, and their target boundary values
Sequentially push intersections and corner points into
F;
Segment irregular boundary \mathbf{V}^i by **F**;
Set $prevDir = i$;
for ($j = 1; j < size(F); j++$) **do**
 $S_j^i = \mathbf{V}^i(F[j], F[j+1])$;
 $S_j^i.dir = direction(F[j], F[j+1])$;
end
for ($j = 1; j <= size(S^i); j++$) **do**
 if ($S^i[j].dir == prevDir \& \& j > 1$) **then**
 $S^i[j] -> S^i[j-1]$;
 end
 else
 if ($dist(S^i[j], S^i[j-1]) < \varepsilon$) **then**
 $S^i[j] -> S^i[j-1]$;
 end
 else
 $prevDir = S^i[j].dir$;
 end
 end
 if ($S^i[j].dir \% 2$) **then**
 $S^i[j].val = Avg(V^i(S^i[j]).y)$;
 end
 else
 $S^i[j].val = Avg(V^i(S^i[j]).x)$;
 end

4.4 Piecewise rectangular stitching

We design a global optimization which combines image stitching and rectangling. Our energy function contains

feature alignment, shape preserving and global similarity constraints that used for stitching, and regular boundary, straight line preserving constraints that rectangling irregular boundaries while avoiding unexpected distortions. The energy terms for stitching have been defined in Section 4.1, and we further define energy terms for irregular boundary rectangling as follows.

Regular boundary preserving. With the piecewise rectangular boundary constraint, we define the regular boundary preserving energy as

$$\phi_r(\mathbf{V}) = \sum_{i=1}^4 \sum_{S_j^i \in \mathfrak{R}(i)} \sum_{V_k \in S_j^i} \left\| \Lambda(S_j^i)^i [\zeta[V_k] V_k + (1 - \zeta[V_k]) (\kappa[V_k] \cdot \eta[V_k])] - S_j^i \cdot \text{val} \right\|^2, \quad (6)$$

where $\mathfrak{R}(i), i = 1, 2, 3, 4$ refer to the set of vertices in *top*, *right*, *bottom* and *left* directions; S_j^i represents all segments in direction i , and $S_j^i \cdot \text{val}$ refers to the values of each target boundary segment; $\zeta[V_k]$ determines the type of vertices: 1 - vertices, 0 - intersections; $\Lambda(S_j^i)$ is the 2×1 matrix, and $\Lambda(S_j^i) = [0 \ 1]$ or $[1 \ 0]$, when S_j^i is horizontal or vertical. For intersection points, we find their neighboring vertices κ that generate the intersections, and their corresponding interpolation weights η , then constrains are imposed on these vertices.

Straight line preserving. To avoid unexpected distortion after warping, we also need to preserve straight lines in panoramas. We use the line preserving term from [22], and the line segments detectors are proposed in [25]. Given the line segments, our energy term is defined as

$$\phi_l(\mathbf{V}) = \sum_{i=1}^N \sum_{l \in L_i} \sum_{j=1}^{M-1} \left\| (1 - \mu) V_{l,0}^i \omega_{l,0}^i + \mu V_{l,M}^i \omega_{l,M}^i - V_{l,j}^i \omega_{l,j}^i \right\|^2, \quad (7)$$

where M is the number of sub-segments for each line segment, and each sample point on the line segment is represented by the bilinear interpolation of the 4 grid vertices. The two end points are represented as $V_{l,0}^i \omega_{l,0}^i, V_{l,M}^i \omega_{l,M}^i$, and the sample point between the end points is $V_{l,j}^i \omega_{l,j}^i$. The linear combination of them can easily preserve the straight lines, and the weight $\mu = j/M$.

With the piecewise regular boundary and straight line preserving constraints, the energy function for content-preserving image stitching with regular boundary can be defined as

$$\Phi(\mathbf{V}) = \Phi_{\text{stitch}}(\mathbf{V}) + \gamma_r \phi_r(\mathbf{V}) + \gamma_l \phi_l(\mathbf{V}), \quad (8)$$

where Φ_{stitch} is the stitching energy function defined in Section 4.1, γ_r and γ_l are weights to control the importance of energy terms. We set $\gamma_r = 10^3$ to ensure the regularity of boundaries. In our experiment, we find that the line preserving is more important than the local shape preserving, thus γ_l is set to be 20 to avoid too much distortions in straight lines.

4.5 Optimization

We first solve optimization for the initial image stitching, which is defined in Equ. 5. However, Equ. 5 only constrains

shape and scale of each mesh, which is not enough for stitching. Thus, we add another term $\phi_p(\mathbf{V}) = W \cdot \|\mathbf{V}_0^0\|^2$ to fix the position of stitched panorama, where \mathbf{V}_0^0 refers to the first vertex(left-top corner) of the first image, and W is a very large weight ($W = 10^4$) to make ϕ_p a hard constraint. Noting that, each energy term is quadratic and variables are mesh vertices of each image, the energy function can be efficiently optimized by solving a linear system. Since this stitching step is only used to get the target rectangle and irregular boundary, we do not need to render the stitching result by warping and blending.

After the irregular boundary extraction, we solve the optimization defined in Equ. 8 which incorporates the regular boundary and straight line constraint into the stitching framework. Compared with initial image stitching, we add another two energy terms, which are also quadratic, thus the optimization can also be efficiently minimized.

With the optimized vertices of each mesh, we further warp each image by texture mapping and remove the visible seam by multibanded blending [19]. For efficiency, we can also simply apply the linear blending, which can works well in most cases. Fig. 1(i) is stitching results constrained by piecewise rectangular boundary. Compared with previous rectangling [3], it makes a better balance between distortion and rectangling.

In this paper, we aim to rectangling the panorama with irregular boundary as much as possible, which means the final shape of the panorama should be as close as possible to a rectangle. Thus, we try to further reduce steps on the piecewise rectangular boundary. We propose a iterative solution which is described in Alg. 3. The first iteration has been accomplished by the optimization above, see Fig. 2(f), and we calculate the energy values E_0 using the optimized vertices. Then we iteratively find the optimal solution, that can preserve regular boundary as much as possible while avoid unwanted distortion. In the following iteration, for each step, we first analyze feature points and lines detection results near the boundary segments connected by the step, and when there are some features and lines, the step cannot be removed, see Fig. 1(h), we preserve the two steps because of the features distributed in the roof and ground. When feature and lines are not salient, such as grass and sky, we further analyze it as follows: for each step, we connect the segments neighboring to it, and reconstruct the S^i , then perform image stitching again, finally we choose to remove the step with the minimum energy value E . In each iteration, the threshold $\sigma = |E_t - E_0|/20$, according to many experiments. When the energy value $E_t - E_0 > \sigma$, it means that the distortion in this iteration is not acceptable. Thus the iteration stops, and we finally get the optimal solution for the piecewise rectangling. Actually, the panorama rectangling proposed by He et al. [3] can be classified as a special case of our piecewise rectangling, when there is no steps in the target boundaries. Fig. 2 (e) is the rectangling result by our method when all steps are removed, and there exists too much distortions in the bottom-right side. Compared with He et al.'s [3] result in Fig. 2 (d) which contains holes and distortions, our rectangling result is better. Fig. 2(f-i) are results of piecewise rectangling in each iteration, and the top-right corner shows the shape of target regular boundary. Results show that each iteration can make the boundary

of panorama be closer to a rectangle, and finally we get panorama with optimal piecewise rectangular boundary and unnoticeable distortions.

Algorithm 3: Iterative piecewise rectangling stitching

```

Input: Source images,  $S$  refers to segments of the
piecewise rectangular boundary in 4 directions,
and  $P$  represents steps that connect all
segments
Output: Stitching result with optimized regular
boundary
Stitching with  $S$  as boundary constraints;
 $E_0 = \Phi(V)$ ,  $V$  is the optimized vertices;
while (1) do
     $Idx = 0, E_t = 10^6;$ 
    for ( $k = 0; k < size(P); k++$ ) do
        segments connected by  $P[k]$ ;
        reconstruct  $S$ ;
        Stitching with  $S$  as boundary constraints;
         $E = \Phi(V)$ ;
        if ( $E < E_t$ ) then
             $| Idx = k;$ 
             $| E_t = \Phi(V);$ 
        end
    end
    if ( $(E_t - E_0) < \sigma$ ) then
        remove  $P[Idx]$ ;
         $E_0 = E_t$ ;
    end
    else
        | break;
    end
    if  $size(P) == 0$  then
        | break;
    end
end

```

5 RESULTS AND APPLICATIONS

In this section, we show a variety of panoramic images by image stitching with regular boundary constraint, and applications that benefit from our approach. Then we further give performance and limitation of our method. In this paper, we use the dataset provided by Chen et al. [4] for image stitching, and the data for video stitching is from Perazzi et al.'s paper [17]. For better exposition, we only provide input for examples provided by ourselves.

5.1 Results

Fig. 3 is the comparison of our method with He et al.'s method [3]. The left initial stitching is the first step of our method. For fair comparison, we also take it as the input of He et al.'s method. As shown in the comparison, the main difference between the two method is the number of mesh used in the global warping. Actually, it is hard to place mesh on images with irregular boundary, and the boundary of the mesh always contain some holes(see bottom side of (a) and (b)), which will finally degrade the quality of the final rectangular panorama, see the zoom-in view in (c). In

addition, He et al.'s method treat stitching and rectangling as two individual processes, thus cannot well preserve the local and global structure of the panorama. In our method, the meshes are placed on the each rectangular images, and the warping are guided by the global optimization which combines stitching and rectangling constraints, thus can produce stitching with regular boundaries while reducing the local and global distortion.

Fig 4 gives comparison with state-of-the-art methods in terms of line preserving. In Chen et al.'s method [4], their line segment detection is used for global feature preserving, like scale and rotation, but they cannot preserve straight lines, as shown in (a). He et al.'s method is limited to the input, and when the input panorama fails to preserve straight lines, their method also fails, see the arrows in (b). (c) and (d) are the initial piecewise rectangular stitching results with and without line preserving, and results show that our method can well preserve straight line in our optimization framework. (e) is the final result after several iterations, which not only preserves lines, but avoid unexpected distortions.

Fig. 5 gives results and comparison of stitching with missing contents in the scene. We provide two groups of experiments to show the effectiveness of our method in challenging cases. (a) is the initial stitching results, which is also the input of He et al.'s [3] method. (b) and (c) show the meshes after initial stitching and the extracted irregular boundaries. (d) and (e) are the rectangular stitching results by He et al.'s and our method. Although both of them has severe distortions, our result is more reasonable and visual pleasing. In addition, the result by He et al.'s method has holes, due to the drawbacks of their mesh. (f) is our piecewise rectangling result, which is the optimal panorama with less distortion, and can preserve the content of panorama in the rectangular windows as much as possible.

Fig. 6 shows comparison with image completion. (a) is the initial stitching result. By completing holes in (a) using Huang et al.'s [30] method, we get rectangular panorama as shown in (c). Zoom-in view in (c) shows that the completion method is limited to synthesize semantic contents. (b) is the piecewise rectangling method, and our method tries the best to preserve regular boundaries while preventing unwanted distortions. Based on our result, image completion can be used to synthesize the regular hole on the left, result in (d) shows that the combination of our method and completion is successful.

Fig. 7 gives results of challenging cases, and each case is very different from common examples. The first row is results of initial stitching result with irregular boundaries, and the second row shows our piecewise rectangling panorama. With the piecewise rectangular boundaries, the panorama can be easily cropped and completed, thus can improve the visual effects and user experience of panorama.

5.2 Applications

5.2.1 Selfie expansion

Recent years, with the fast development of intelligent devices such as smart phones, pad etc., selfies have become more and more popular. In general, selfie images are mostly shot by mobile phones by holding them or fixing them to

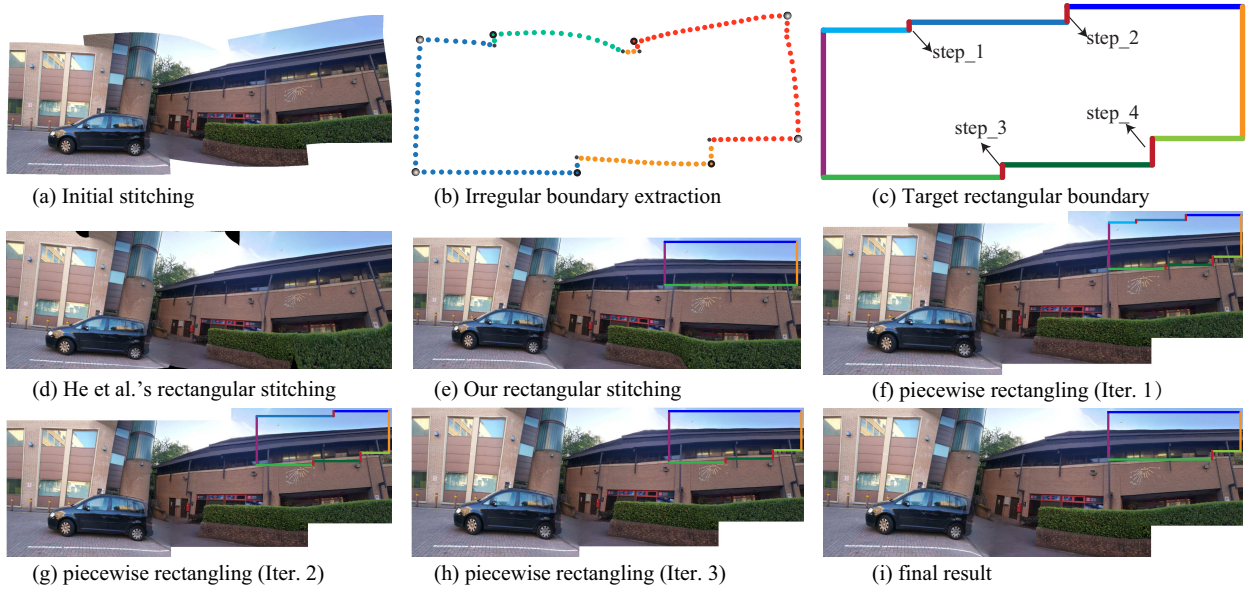


Fig. 2. Piecewise rectangling in image stitching. (a) Initial stitching result with irregular boundary. (b) Irregular boundary extraction. (c) Target boundaries estimation. (d) He et al.'s [3] rectangular stitching result. (e) Our rectangular stitching result. (f i) stitching results by iterative piecewise rectangling, and (i) is our final stitching result.

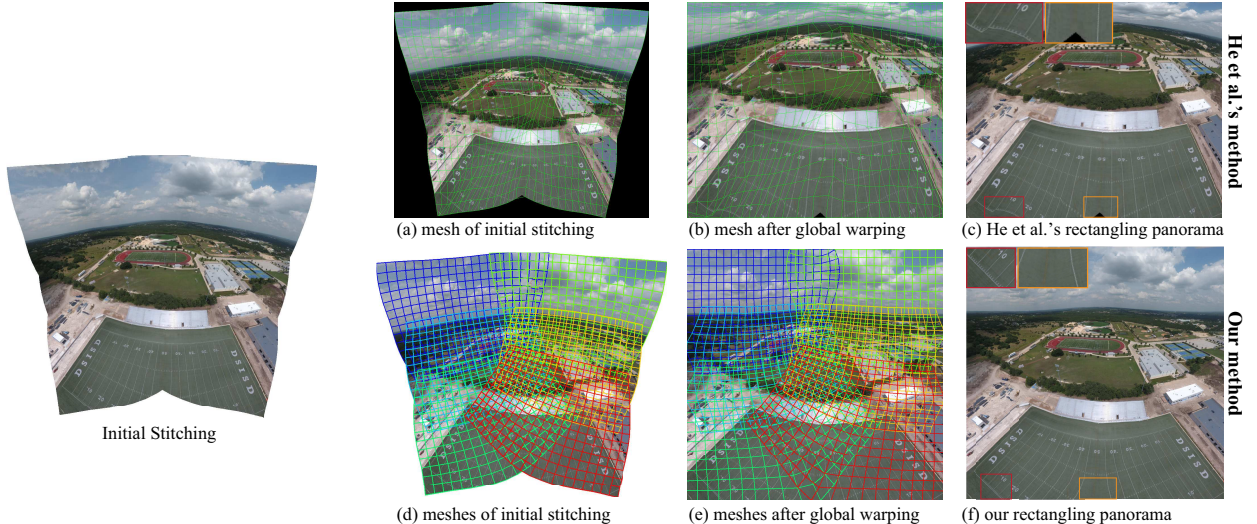


Fig. 3. Comparison with He et al.'s method [3]. The initial stitching is the first step of our method, which is also the input of He et al.'s method [3]. For He et al.'s method: (a) mesh of on the input image; (b) mesh after global warping; (c) final rectangular panorama. For our method: (d) meshes of our initial stitching; (e) meshes after the global warping; (f) our rectangular panorama.

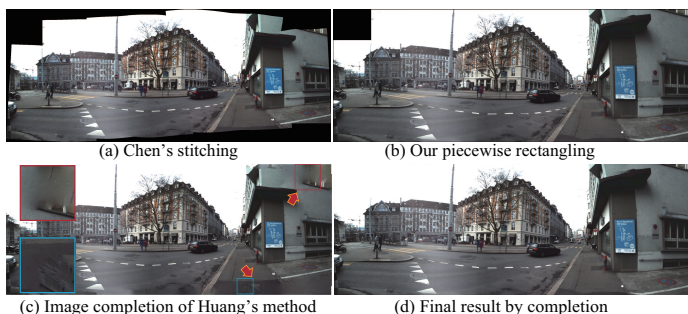


Fig. 6. Comparison with image completion. (a) is the result of initial stitching. (b) shows our piecewise rectangling panorama. (c) is the result by Huang et al.'s [30] image completion. (d) our final result which is generated by completing holes in (b).

selfie sticks. Since the camera is very close to people, the selfie photos are always limited by the field-of-view, thus reducing the fun of selfies. To produce selfies with large field-of-view, we apply our image stitching to producing selfie panorama. Actually, the front-facing camera which is used for selfie shooting, can not shoot a panorama view. We first take photos of the panorama view using the back camera, then shot our portrait using the front-facing camera on the background of the panorama. See Fig. 9, (a) is the input, which contains photos for the panorama background, and the portrait photo. (b) is the result by Chen et al.'s stitching [4], which contains irregular boundaries. (c) is result by our method. However, the portrait is distorted too much. We first detect the face the portrait photo, and modify

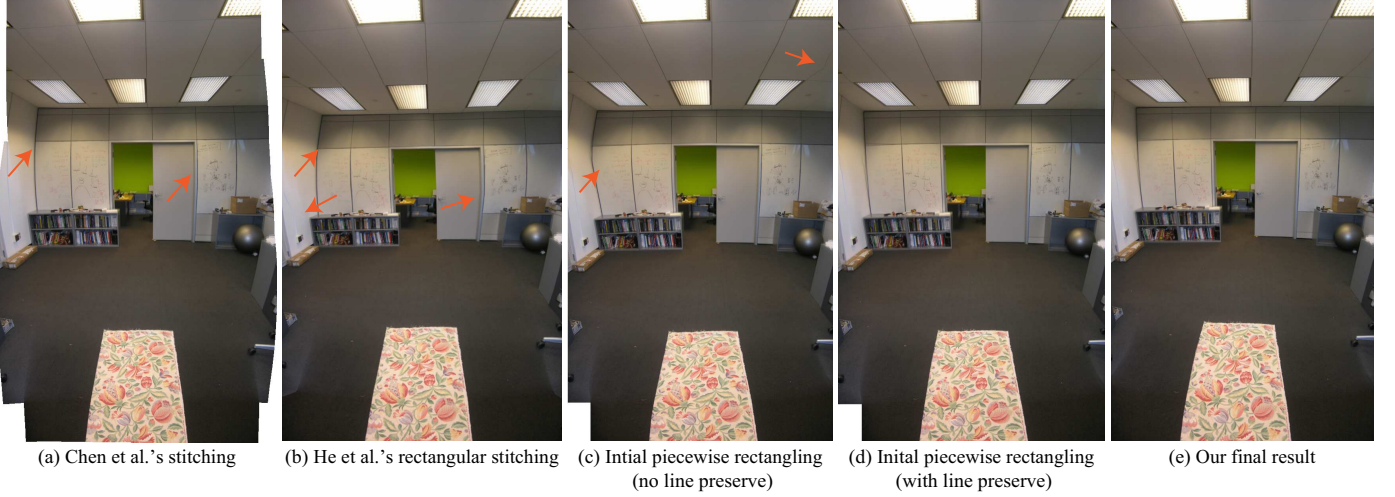


Fig. 4. Comparison with state-of-the-art methods. (a) Chen's [4] stitching with global prior. (b) He et al.'s [3] rectangling stitching. (c) and (d) are Our piecewise rectangling results in the 1st iteration with and without line preserving). (e) our final stitching results after several iterations.

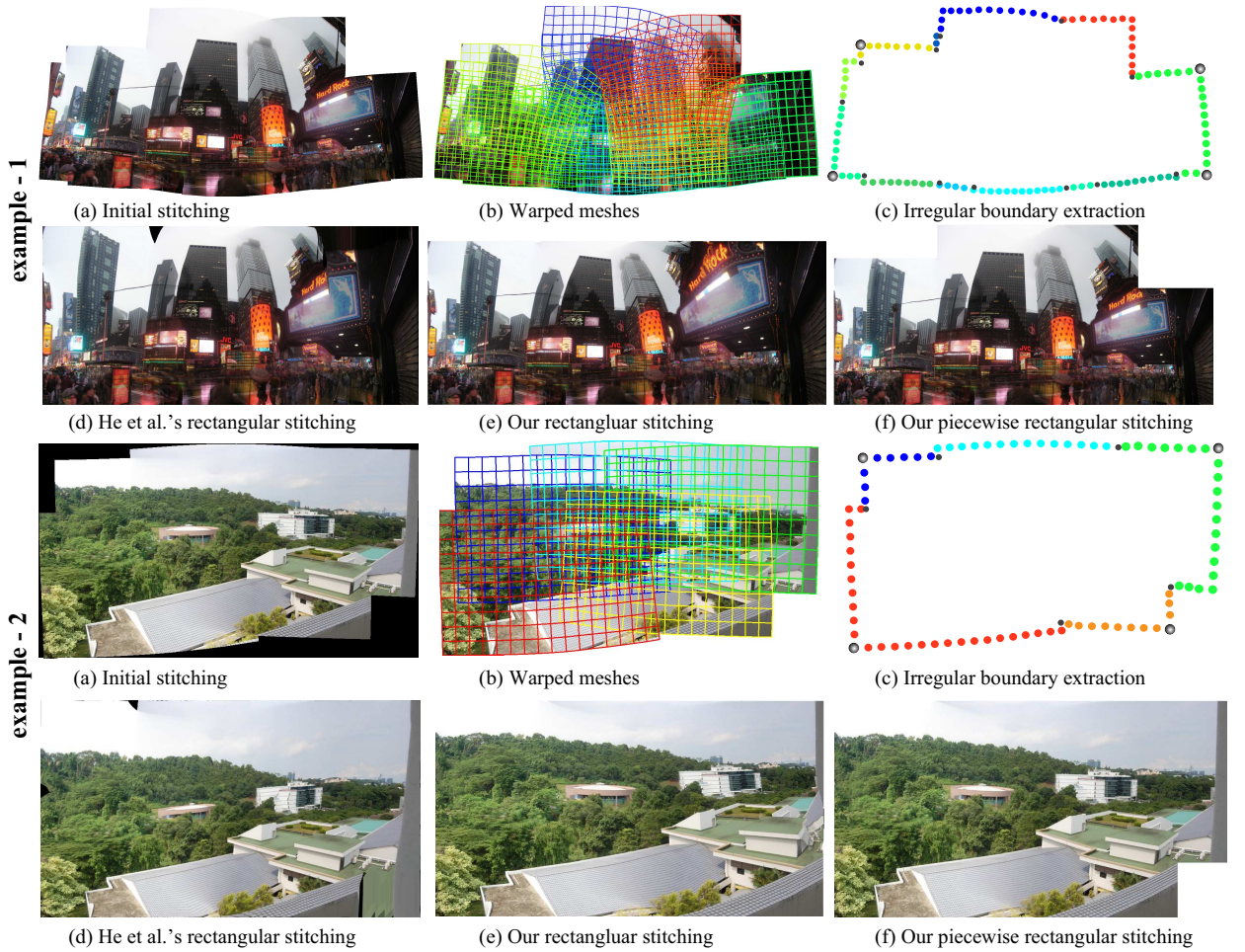


Fig. 5. Results and comparison of stitching with missing contents. There are two sets of results, and each set is as follows: (a) Initial stitching result with irregular boundaries. (b) Warped meshes of initial stitching. (c) Irregular boundary extraction. (d) and (e) are rectangling stitching by He's [3] and our method respectively. (f) our piecewise rectangular stitching result.



Fig. 8. More results of our method. The initial stitching is traditional method without the regular boundary constraint, and final results are obtained by our rectangular stitching.



Fig. 7. Results of challenging cases. The 1st row shows Initial stitching results with irregular boundaries, and the 2nd row shows results of our piecewise rectangling stitching.

Equ. 2 as

$$\phi_s(\mathbf{V}) = \sum_{i=1}^N \sum_j \alpha_j^i \|V_j^i - V_1^i - \xi \mathbf{R}(V_0^i - V_1^i)\|^2, \quad (9)$$

where alpha_j^i refers to the saliency value of vertex V_j^i , we give a big value ($\text{alpha}_j^i=20$) for vertices in the face region, and 1 for others. By preserving the shape of mesh in the face region, the stitching result is much more visual pleasing, as shown in (d).

5.2.2 Rectangling Video Panorama

We further apply our method to videos. Actually, it is difficult to stitch the videos from independent hand-held cameras, and rectangling them is even more challenging. Because the regular boundary in each frame is different and the temporal coherence is difficult to maintain due to the shaking in each video. Inspired by Perazzi et al.'s [17] work, we aim to rectangling panorama videos from unstructured camera arrays, which are fixed on a rag. For fixed camera configurations, the warping parameters for stitching in each frame are nearly invariant. For temporal coherence, we propose a simple and effective scheme as follows. We first divide videos into several blocks (1 block=30 frames), and neighboring block has 10 frames overlap. For each block,

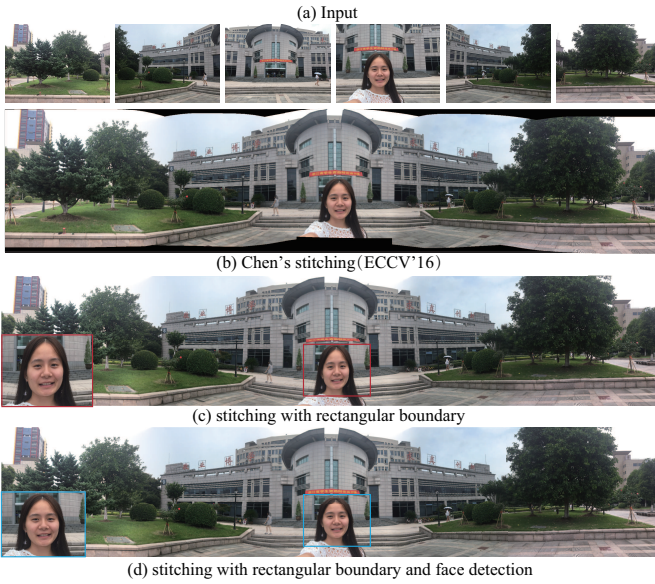


Fig. 9. Application of *Selfie* panorama. (a) Initial stitching results with irregular boundaries. (b) Results of our stitching with regular boundary, which distorts the human face. (c) Results of our stitching with regular boundary and face detection, which can avoid the unwanted face distortion.

we compute the stitching result for the first frame, and the warping parameters are used for other frames. For the overlapping part, the warping parameters are linear combination of neighboring blocks. Fig. 10 shows result two sets of results, and each set shows video panoramas of different frames by Perazzi et al.'s [17] and our method. Comparison shows that our method is effective to rectangling video panorama shot by fixed camera arrays.

5.3 Performance

We report performance of our method on a Intel Core i7 8550U 1.99GHz laptop with 16G RAM for examples in this paper. Take Fig.1 for example, the input contains 5 images, and size of each image is 800×600 , the initial stitching cost 0.76s, which includes feature matching, energy construction and optimization. Then, the stitching with rectangular boundary constraint cost 0.49s, which include the irregular boundary extraction, boundary constraint construction and iterative optimization. Finally, with the warped vertices, texture mapping and blending are performed, and the time cost is 2.15s. In our two-step optimization, the energy terms are similar, thus we construct them only once. In addition, the energy terms are quadratic, thus can be efficiently solved. For our iterative optimization in the piecewise rectangling, results in each iteration are similar, thus we apply conjugate gradient method, which takes result of last iteration as input, thus can solve the optimization more efficiently.

5.4 Limitations

Due to the free movement of hand-held cameras, panorama images has irregular boundaries and missing contents. Our piecewise rectangling stitching can effectively rectify these problems by warping-based optimizations with regular boundary constraints. However, there are still some

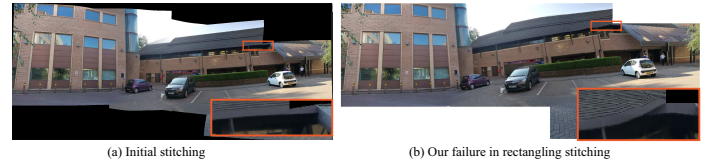


Fig. 11. Failure case: when there is strong structure in the intersection of meshes, our method may fail to preserve the structure.

limitations: (1) Similar to most warping-based methods, our method cannot well preserve all lines when there are many lines in local regions. (2) Our method may fail when there is strong structure near the intersection of neighboring meshes. See Fig. 11, the zoom-in view show that, our piecewise rectangling scheme may introduce unwanted distortion in order to preserve the rectangular boundaries.

6 CONCLUSION

In this paper, we have proposed an efficient approach for content-preserving stitching with the regular boundary constraint, thus can generate panorama images with regular boundaries. Our main contribution is to propose a global optimization which incorporates the regular boundary constraint in the framework of image stitching. Based on the traditional stitching with irregular boundaries, we analyze the warped meshes and extract the outer boundary by the polygon boolean operation. With the outer boundary, we setup the piecewise rectangular boundary constraint for the content-preserving stitching. Compare with He et al.'s panorama rectangling, our method is more robust and effective. Especially for panoramic scenes with missing content, our piecewise rectangling can not only regularize the stitching boundary as-much-as-possible, but avoids unwanted distortions. Experimental results and comparisons show that our method is effective and better than state-of-the-art methods. Some challenging examples show the robustness and practicability. We further apply our method to *Selfie* panorama and video stitching, which demonstrate the versatility of our approach.

In the future, we will consider more features to improve the performance of panorama boundary rectangling, such as structure, saliency, scene analysis etc. For video stabilization and stitching, the warping-based method may also introduce the irregular boundaries. Regularizing the boundary of warped videos can preserve more content in a cropping window and improve the viewing experiences. However, for videos shot by freely moving hand-held cameras, it is difficult to define the regular boundary constraint, and maintain the spatial-temporal coherence. We leave these problems as our future work.

ACKNOWLEDGMENTS

The authors would like to thank...

REFERENCES

- [1] S. Yen, H. Yeh, and H. Chang, "Progressive completion of a panoramic image," *Multimedia Tools Appl.*, vol. 76, no. 9, pp. 11 603–11 620, 2017.

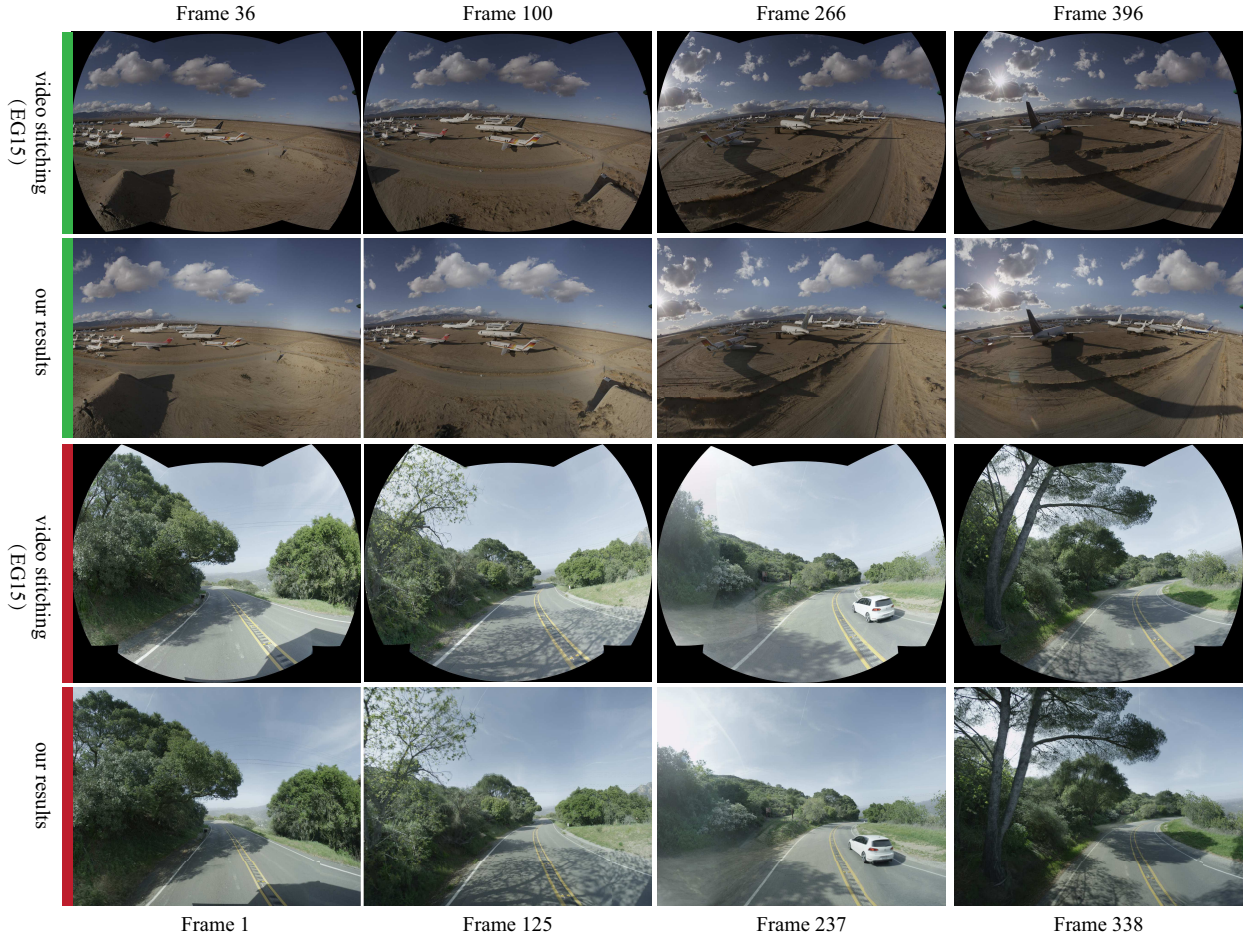


Fig. 10. Application of rectangling video panorama. We give two examples, and each example shows stitching results of 4 different frames using Perazzi et al.'s [17] method and our rectangling respectively.

- [2] C. Barnes, E. Shechtman, A. Finkelstein, and D. B. Goldman, "Patchmatch: a randomized correspondence algorithm for structural image editing," *ACM Trans. Graph.*, vol. 28, no. 3, pp. 24:1–24:11, 2009.
- [3] K. He, H. Chang, and J. Sun, "Rectangling panoramic images via warping," *ACM Trans. Graph.*, vol. 32, no. 4, pp. 79:1–79:10, 2013.
- [4] Y. Chen and Y. Chuang, "Natural image stitching with the global similarity prior," in *Computer Vision - ECCV 2016 - 14th European Conference, Amsterdam, The Netherlands, October 11-14, 2016, Proceedings, Part V*, 2016, pp. 186–201.
- [5] R. Szeliski, "Image alignment and stitching: A tutorial," *Foundations and Trends in Computer Graphics and Vision*, vol. 2, no. 1, 2006.
- [6] M. Brown and D. G. Lowe, "Automatic panoramic image stitching using invariant features," *International Journal of Computer Vision*, vol. 74, no. 1, pp. 59–73, 2007.
- [7] J. Gao, S. J. Kim, and M. S. Brown, "Constructing image panoramas using dual-homography warping," in *IEEE Conference on Computer Vision and Pattern Recognition (CVPR)*, 2011, pp. 49–56.
- [8] J. Zaragoza, T. Chin, Q. Tran, M. S. Brown, and D. Suter, "As-projective-as-possible image stitching with moving DLT," *IEEE Trans. Pattern Anal. Mach. Intell.*, vol. 36, no. 7, pp. 1285–1298, 2014.
- [9] C. C. Lin, S. U. Pankanti, K. N. Ramamurthy, and A. Y. Aravkin, "Adaptive as-natural-as-possible image stitching," in *IEEE Conference on Computer Vision and Pattern Recognition (CVPR)*, 2015, pp. 1155–1163.
- [10] S. Li, L. Yuan, J. Sun, and L. Quan, "Dual-feature warping-based motion model estimation," in *2015 IEEE International Conference on Computer Vision, ICCV 2015, Santiago, Chile, December 7-13, 2015*, 2015, pp. 4283–4291.
- [11] C. Chang, Y. Sato, and Y. Chuang, "Shape-preserving half-projective warps for image stitching," in *2014 IEEE Conference on Computer Vision and Pattern Recognition, CVPR 2014, Columbus, OH, USA, June 23-28, 2014*, 2014, pp. 3254–3261.
- [12] F. Zhang and F. Liu, "Parallax-tolerant image stitching," in *2014 IEEE Conference on Computer Vision and Pattern Recognition, CVPR 2014, Columbus, OH, USA, June 23-28, 2014*, 2014, pp. 3262–3269.
- [13] K. Lin, N. Jiang, L. Cheong, M. N. Do, and J. Lu, "SEAGULL: seam-guided local alignment for parallax-tolerant image stitching," in *Computer Vision - ECCV 2016 - 14th European Conference, Amsterdam, The Netherlands, October 11-14, 2016, Proceedings, Part III*, 2016, pp. 370–385.
- [14] J. Li, Z. Wang, S. Lai, Y. Zhai, and M. Zhang, "Parallax-tolerant image stitching based on robust elastic warping," *IEEE Trans. Multimedia*, vol. 20, no. 7, pp. 1672–1687, 2018.
- [15] B. He and S. Yu, "Parallax-robust surveillance video stitching," *Sensors*, vol. 16, no. 1, p. 7, 2016.
- [16] X. Yin, W. Li, B. Wang, Y. Liu, and M. Zhang, "A novel video stitching method for multi-camera surveillance systems," *TIIS*, vol. 8, no. 10, pp. 3538–3556, 2014.
- [17] F. Perazzi, A. Sorkine-Hornung, H. Zimmer, P. Kaufmann, O. Wang, S. Watson, and M. H. Gross, "Panoramic video from unstructured camera arrays," *Comput. Graph. Forum*, vol. 34, no. 2, pp. 57–68, 2015.
- [18] D. Anguelov, C. Dulong, D. Filip, C. Früh, S. Lafon, R. Lyon, A. S. Ogale, L. Vincent, and J. Weaver, "Google street view: Capturing the world at street level," *IEEE Computer*, vol. 43, no. 6, pp. 32–38, 2010.
- [19] Z. Zhu, J. Lu, M. Wang, S. Zhang, R. R. Martin, H. Liu, and S. Hu, "A comparative study of algorithms for realtime panoramic video blending," *IEEE Trans. Image Processing*, vol. 27, no. 6, pp. 2952–2965, 2018.
- [20] X. Meng, W. Wang, and B. Leong, "Skystitch: A cooperative multi-uav-based real-time video surveillance system with stitching," in *Proceedings of the 23rd Annual ACM Conference on Multimedia Conference, MM '15, Brisbane, Australia, October 26 - 30, 2015*, 2015, pp. 261–270.

- [21] M. A. El-Saban, M. Ezz, A. Kaheel, and M. Refaat, "Improved optimal seam selection blending for fast video stitching of videos captured from freely moving devices," in *18th IEEE International Conference on Image Processing, ICIP 2011, Brussels, Belgium, September 11-14, 2011*, 2011, pp. 1481–1484.
- [22] K. Lin, S. Liu, L. Cheong, and B. Zeng, "Seamless video stitching from hand-held camera inputs," *Comput. Graph. Forum*, vol. 35, no. 2, pp. 479–487, 2016.
- [23] H. Guo, S. Liu, T. He, S. Zhu, B. Zeng, and M. Gabbouj, "Joint video stitching and stabilization from moving cameras," *IEEE Trans. Image Processing*, vol. 25, no. 11, pp. 5491–5503, 2016.
- [24] Y. Nie, T. Su, Z. Zhang, H. Sun, and G. Li, "Dynamic video stitching via shakiness removing," *IEEE Trans. Image Processing*, vol. 27, no. 1, pp. 164–178, 2018.
- [25] R. G. von Gioi, J. Jakubowicz, J. Morel, and G. Randall, "LSD: A fast line segment detector with a false detection control," *IEEE Trans. Pattern Anal. Mach. Intell.*, vol. 32, no. 4, pp. 722–732, 2010.
- [26] S. Liu, L. Yuan, P. Tan, and J. Sun, "Bundled camera paths for video stabilization," *ACM Trans. Graph.*, vol. 32, no. 4, pp. 78:1–78:10, 2013.
- [27] T. Igarashi, T. Moscovich, and J. F. Hughes, "As-rigid-as-possible shape manipulation," *ACM Trans. Graph.*, vol. 24, no. 3, pp. 1134–1141, 2005.
- [28] T. Igarashi and Y. Igarashi, "Implementing as-rigid-as-possible shape manipulation and surface flattening," *J. Graphics, GPU, & Game Tools*, vol. 14, no. 1, pp. 17–30, 2009.
- [29] F. Martínez, A. J. Rueda, and F. R. Feito, "A new algorithm for computing boolean operations on polygons," *Computers & Geosciences*, vol. 35, no. 6, pp. 1177–1185, 2009.
- [30] J. Huang, S. B. Kang, N. Ahuja, and J. Kopf, "Image completion using planar structure guidance," *ACM Trans. Graph.*, vol. 33, no. 4, pp. 129:1–129:10, 2014.